International Journal of Digital Information and Wireless Communications (IJDIWC) 4(3): 401-407
The Society of Digital Information and Wireless Communications, 2014 (ISSN: 2225-658X)

# Miniaturized Bandstop Filters Using Slotted-Complementary Resonators

Mohammed M. Bait-Suwailam
Department of Electrical and Computer Engineering, College of Engineering
Sultan Qaboos University,
Muscat, Oman
E-mail: msuwailem@squ.edu.om

## ABSTRACT

This paper presents a technique to miniaturize bandstop filters applicable for radio-frequency/microwave applications. The technique comprises the use of small resonant inclusions bridged with a slot, etched from the metallic ground plane underneath the filter's microstrip line segment. Unlike artificial magnetic materials, for instance split-ring resonators (SRRs) that respond to vertical magnetic field, complementary SRRs (CSRRs) resonate upon an excitation of an axial time-varying electric field. Numerical full-wave studies are presented here to validate and proof the proposed concepts. It is found that high miniaturization factors can be achieved for the filters loaded with the proposed slotted complementary resonators in comparison to non-slotted resonators. Furthermore, sensitivity analysis is conducted to study the effect of geometrical parameters of the proposed slotted resonators as well as the effect of the choice of host media on the suppression bandwidth and rejection level of such filters. Miniaturized bandstop filters based on developed slotted-complementary spiral resonators are also proposed and numerically evaluated.

## KEYWORDS

Bandstop filters, complementary-split ring resonators (CSRRs), slotted-CSRRs, miniaturized filters.

## 1 Introduction

Microwave filters are vital building blocks in modern wireless communication systems. Such filters are widely used to either pass particular frequency components or reject spurious modes or harmonics. In particular, microwave bandstop filters are used quite often in cellular base stations, navigation systems and alike. Amongst the available bandstop filters manufacturing technologies, the Microstrip line bandstop filters (BSFs) are indeed more attractive in modern

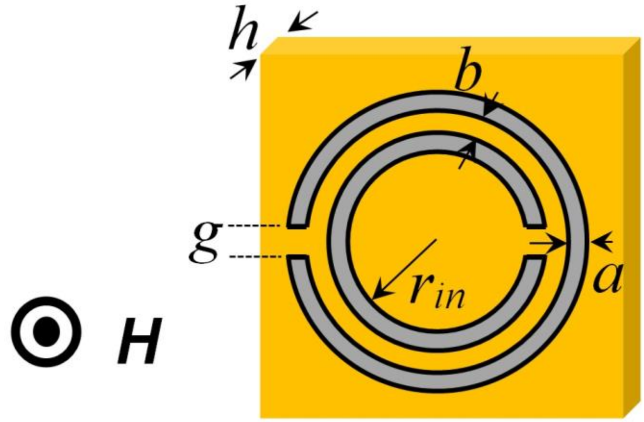


**Fig. 1** A split-ring resonator (SRR) particle with its relevant dimensions. Note that gray area represents metallization.

wireless communication systems due to their low cost and ease of integration with other radio frequency/microwave circuits.

There exists variety of techniques to design microstrip BSFs. One of which is to employ shunt open-circuited resonators that are quarter-wavelength long, which fits more to filter out narrowband signals [1]. However, other techniques, like the use of periodic structures, defected ground plane structure are more desirable for wideband communication systems [2]-[5].

Recently, subwavelength resonators, well-known in literature as *metamaterials*, have received much attention, especially for the synthesis of filters design and harmonics suppression [6]-[8]. For instance, split-ring resonator (SRR) that was originally proposed in 1999 has widely been used to artificially synthesize magnetic materials [9]. Pendry *et. al* in his pioneering work [9] proposed the use of two concentric small metallic rings with opposite cuts (see Fig. 1) to further enhance the magnetic resonance of such rings. By cascading enough periods of aforementioned concentric rings and formed in either periodic or aperiodic fashion, artificial materials can be realized with unique effective magnetic permeability response. When excited with an axial time-varying magnetic field **H** (see Fig. 1), SRRs resonate and hence give rise to an effective magnetic response, $\mu_{\text{eff}}$. It was until that Smith and his ground [10] made the first artificial magnetic material following the hypothetical analysis of Veselago [11] and Pendry to realize materials with unique effective electric and magnetic properties.

It is important to highlight here that at frequencies below the resonance frequency of the SRR inclusion, the effective magnetic permeability becomes positive, while at frequencies above the SRR's resonance, $\mu_{\text{eff}}$ becomes negative. On the other hand, complementary split-ring resonator (CSRR) is the dual-counter part of SRR [12]. In other words, CSRR starts to resonate once excited with an axial time-varying electric field **E**. Based on Babenit's principle [13], this means that CSRRs give rise to an effective electric response, $\varepsilon_{\text{eff}}$. CSRRs are in fact achieved by replacing the metallic rings of SRRs with apertures (i.e., slotted rings) and surrounding free-space region nearby SRR inclusion is replaced with metallic plate.

Fig. 2 (a) depicts a unit cell of CSRR inclusion. For simplicity, a square shaped resonator is shown. At resonance, the inductance from the inclusion's metals balances the capacitance between the etched rings of the resonator. Recently, slotted-CSRR inclusions were proposed to mitigate space wave coupling effect between microstrip patch antennas [14]. In Fig. 2 (b), a modified resonator is proposed through the use of two collinear CSRRs connected through a compact slit. The slit (or bridging slot) provides significant advantage in enhancing the bandwidth of the proposed stopband filter.

This paper aims to explore the application of such slotted resonators as particles to enhance performance of bandstop filters. While in [15] the aforementioned application was briefly highlighted, herein, more analyses are devoted to thoroughly investigate the effect of geometrical parameters as well as the applied host medium of the proposed slotted complementary resonators on the suppression band of the filters. Furthermore, techniques to further miniaturize bandstop filters are proposed, and numerically assessed.

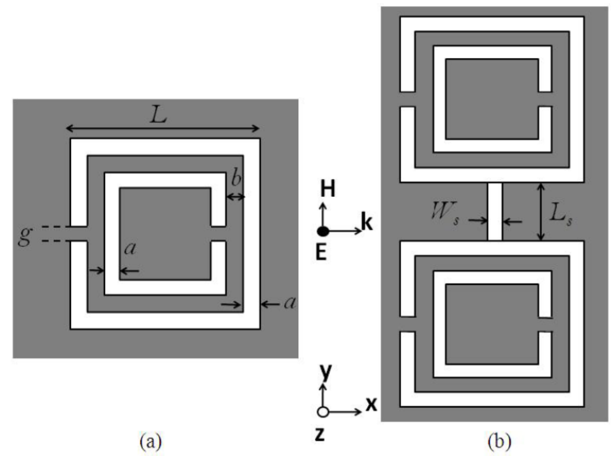


**Fig. 2** (a) CSRR unit cell, and (b) the proposed slotted-CSRR inclusion. Note that gray area represents metallization.

## 2 Design of bandstop filters based on Slotted Complementary Resonators

Both SRR and its dual counterpart (CSRR) (see Fig.2(a)) have widely been applied as building blocks in variety of engineering applicants, including filtering and harmonics rejection [16]. In fact, the resonance frequency of either SRR or CSRR inclusions can be estimated analytically using quasi-static electromagnetic theory [6] or alternatively numerically using full-wave characterization methods. At resonance, SRR or CSRR behaves as an *LC* resonant tank circuit. In this paper, more emphasis is devoted to the numerical modeling aspects of bandstop filters loaded with CSRRs and the proposed slotted resonators. Two versions of slotted resonators are proposed and studied here, namely: slotted-CSRRs and slotted-spiral resonators (S-SRs).

### *A. Slotted-CSRRs based filters*

The type of filter (S-CSRRs) is based on a modified version of CSRRs. The new resonator consists of two CSRRs bridged with a slot of length $L_s$ and width $W_s$ as shown in Fig. 2(b). For simplicity, a square shaped resonator is adopted. A wide stopband rejection of signals is achieved by linearly cascading the suppression band of both CSRRs and the slot. By cascading several varied in size S-CSRRs, a wide stopband behavior is attainable. Fig. 3 shows the bandstop filter comprises a transmission line segment of width 2.88 *mm* for an impedance of 50 Ω. The proposed resonator (slotted-CSRR) has the following geometrical parameters (see Fig. 1): $L$ = 4 *mm*, $a$ = $b$ = $g$ = 0.2 *mm*, $L_s$ = 2 *mm*, and $W_s$ = 0.35 *mm*, where a dielectric substrate ($\varepsilon_r$ = 3.48, $tan\ \delta$ = 0.004) with a thickness of 1.27 *mm* is used. In this study, more than one S-CSRR unit cell is used. This helps to provide strong suppression (zero transmission) when capturing the transmission coefficient, $S_{21}$, between two ports of a transmission line segment as indicated in Fig. 3. The periodicity (separation distance between each successive S-CSRR inclusion) is maintained constant at 1 *mm* for ease of manufacturing.

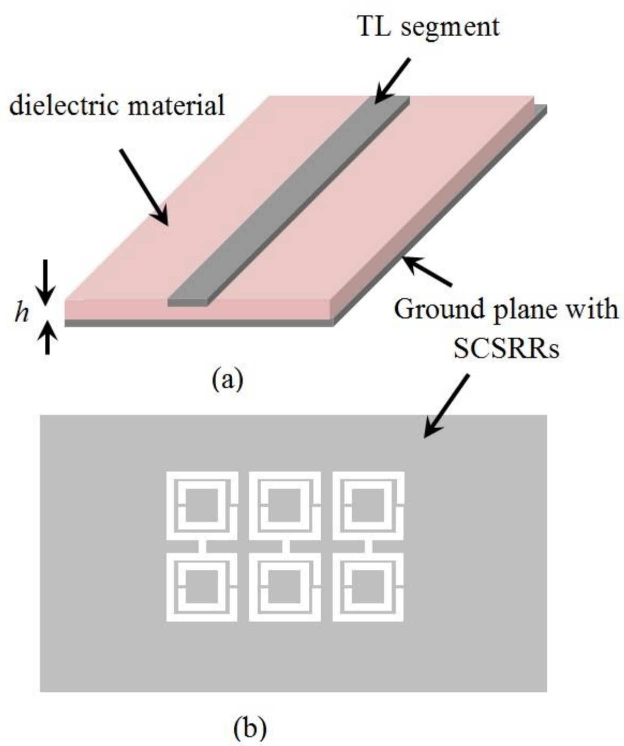


**Fig. 3** (a) 3D view of the bandstop filter with SCSRRs etched from ground plane; (b) bottom view of the bandstop filter with slotted-CSRRs etched from the ground plane.

To demonstrate the effectiveness of the slot of the S-CSRR cell in the proposed filter, comparison is made to classical CSRR cell. In order to keep the resonance of CSRR lies within the S-CSRR cell, a bigger CSRR cell is therefore needed. For instance, to achieve bandstop suppression at around 5 GHz, the CSRR unit cell would require an outer area of 4.5 x 4.5 $mm^2$. Other complementary configurations are also shown for comparison purposes. As can be seen from Fig. 4, a suppression bandwidth ($S_{21}$ < -15 dB) of more than 1 GHz resulted when using 3 cells of S-CSRRs. Furthermore, a wider suppression band can be achieved by increasing the number of S-CSRR cells. The classical CSRRs have narrowband suppression in comparison to the proposed filter. The use of the S-CSRR without the slits resulted in narrowband suppression as expected.

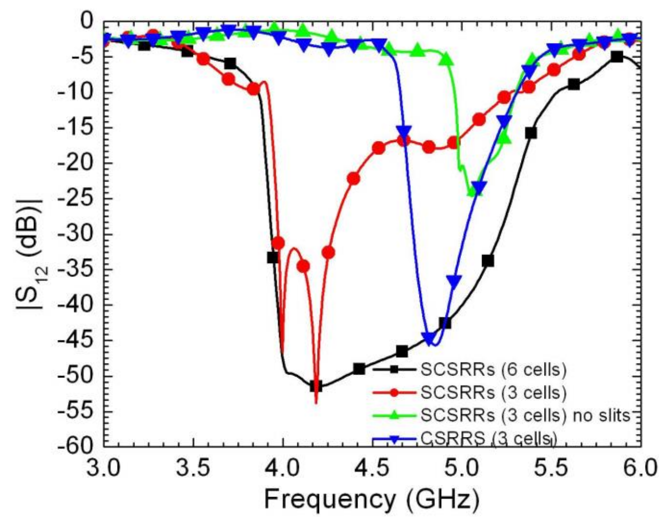


**Fig. 4** Simulated transmission coefficient, $S_{21}$, for the bandstop filter with the proposed slotted-CSRRs, and compared to a bandstop filter with classical CSRR inclusions.

A parametric study of the effect of the slot on the filter suppression capability is shown next. The slot width, $W_s$, is varied and the transmission coefficient of the bandstop filter is numerically computed. Fig. 5 depicts the transmission coefficient for the filter when varying the width of the slot. It can be inferred from Fig. 5 that a decrease in the slot width, $W_s$, increases the capacitance of the slit and hence causes the rejection band of the filter to shift to lower frequencies.

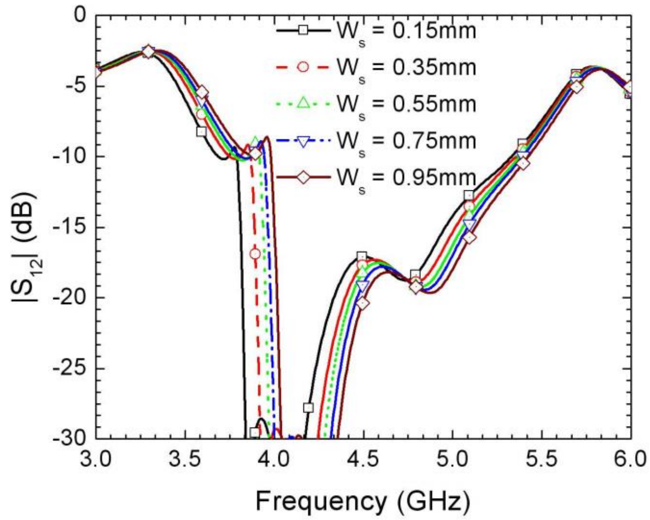


**Fig. 5** A parametric study illustrates the effect of the S-CSRR slot width, $W_s$, on the rejection band of the filter.

The attenuation coefficient for the proposed filter with S-CSRRs is numerically computed and compared with CSRRs (without the slit). As can be seen from Fig. 5, a wider attenuation band resulted for the proposed filter when compared with CSRRs. This demonstrates the sharp and strong suppression of the proposed bandstop filter.

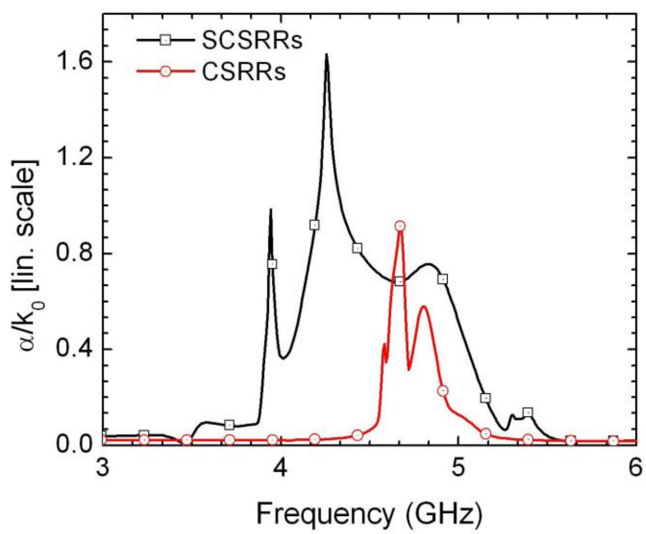


**Fig. 6** Attenuation coefficient for the proposed filter with S-CSRRs and compared with CSRRs filter (without the slot).

## B. *Slotted-Spirals based filters*

The slotted-spiral resonators follows similar structural feature as that S-CSRRs. It is understood that the capacitance of a metallic spiral resonator is almost fourth of that of a split-ring resonator. In other words, the capacitance of complementary spiral resonator (CSR) is almost twice that capacitance of the CSRR. Thus, more miniaturization is achieved with the use of spiral resonant inclusions rather than the SRRs. In this paper, slotted-spirals, as will be shown later, are indeed good candidates to provide size reduction of the bandstop filters.

To better understand the physical behavior of slotted-CSR, bandstop filters based on CSRs are studied first. Fig. 7 depicts CSR unit cell and the proposed (S-CSR) inclusion.

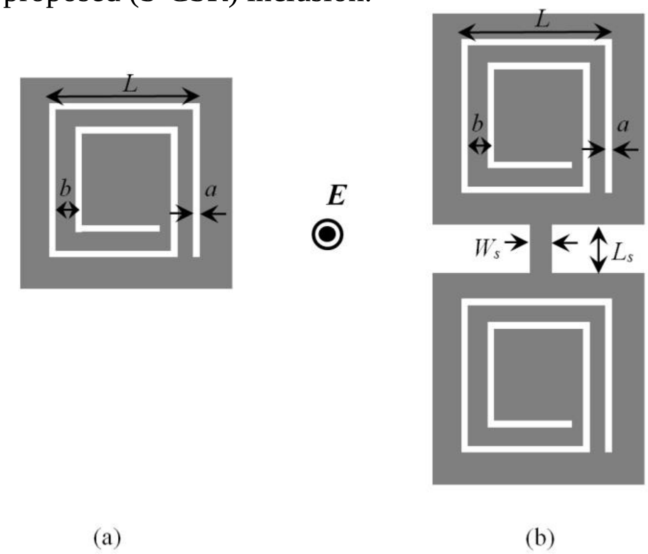


**Fig. 7** (a) Complementary spiral resonator (CSR) unit cell with its relevant dimensions, and (b) the proposed slotted-CSR unit cell. Note that gray area represents metallization.

The geometrical dimensions of the CSRs are: side length $L$ = 6 *mm*, $a$ = 0.2 *mm*, $b$ = 0.4 *mm*, where a dielectric substrate ($\varepsilon_r$ = 3.48, *tan* $\delta$ = 0.004) with a thickness of 1.27 *mm* is used. The periodicity, that is separation distance between adjacent CSR elements, was chosen as 0.4 *mm*. Three CSR unit cells are placed adjacent to each other and etched out from metallic ground plane beneath a TL segment of width 1.18 *mm* in order to match it to 50 Ω, as shown in Fig. 8. Two ports were used to numerically compute the transmission coefficient, $S_{21}$.

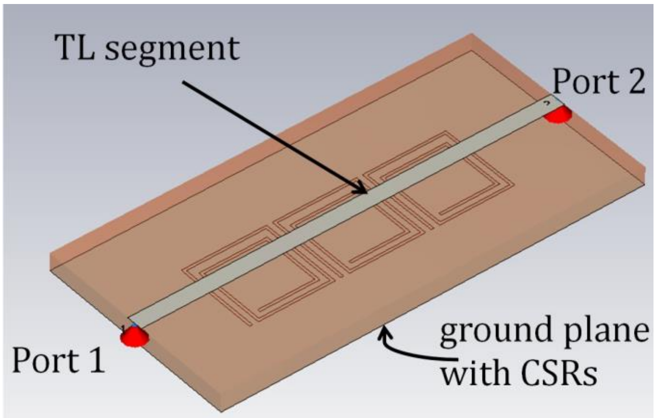


**Fig. 8** 3D view of the bandstop filter with complementary spiral resonators etched out from metallic ground plane. Note that TL segment is matched to 50Ω.

Fig. 9 depicts the transmission coefficient of the bandstop filter with three CSRs etched out from the ground plane. A narrowband suppression for the filter can be seen around 2.45 GHz, that makes such filters suitable for wireless local area networks to reject any kind of electromagnetic noise around that particular frequency. It is indeed expected to achieve such narrowband behavior from such resonators, due to their inherent high quality factors. Furthermore, Fig.9 shows the possibility of miniaturizing the filter by just changing the host medium above the ground plane with the etched CSRs, from $\varepsilon_r = 3.48$ to $\varepsilon_r = 10.2$, the suppression band is shifted to lower frequencies, around 1.25 GHz in addition to another suppression band around 3.2 GHz.

Fig. 10 shows snapshots for the computed surface current distribution along the metallic ground layer of this filter with CSRs. It is observed that high current concentration is observed at the resonant frequencies of the CSRs that lie within the suppression band of the filter, at 1.2 GHz and 3.0 GHz as shown in Figs. 10(a) and (c). On the other hand, low current circulates around the resonators (see Fig. 10(b)) at the non-resonant frequency, 2.5 GHz as expected. Note that these snapshots correspond to the filter with a host dielectric medium, $\varepsilon_r = 10.2$, tanδ = 0.0023.

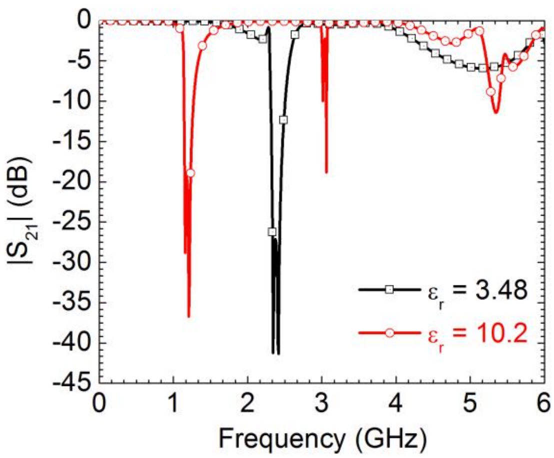


**Fig. 9** Simulated transmission coefficient, $S_{21}$, for the filter with CSRs. Note that no slits are presented for the CSRs.

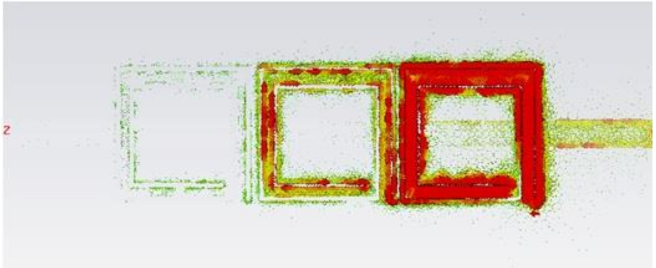

(a)

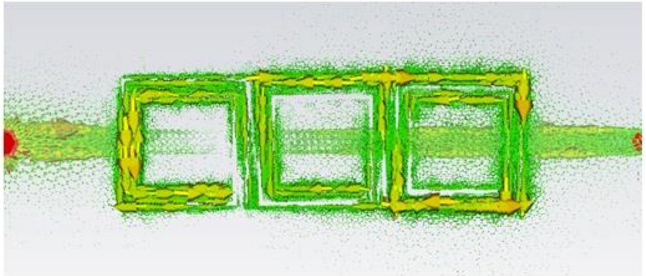

(b)

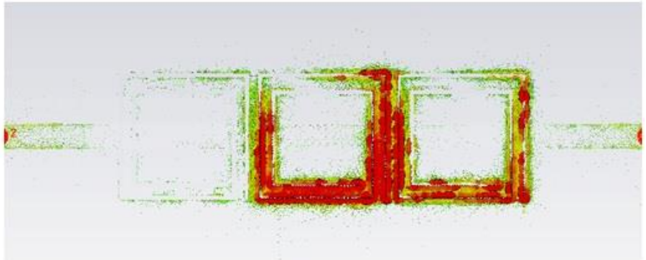

(c)

**Fig. 10** Snapshots for simulated surface current distribution along the vicinity of the metallic ground plane of the bandstop filter with CSRs at various frequencies: (a) 1.2 GHz, (b) 2.5 GHz, and (c) 3.0 GHz. Note that no slits are presented for the CSRs.

The effect of the bridged slot between resonant CSRs is investigated next on the suppression band of bandstop filters. Similar model (see Fig. 11) to that presented in Fig. 8 is numerically studied and simulated to extract the suppression band of the filer. The transmission coefficient, $S_{21}$, is computed by considering two ports at the edges of a TL segment of width 3.5 *mm* for proper match to a 50-Ω impedance. The width and length of the slot, that is used to bridge two CSRs, is chosen as $W_s$ = 0.15 *mm* and $L_s$ = 2 *mm*, while the length of the two identical CSRs is taken as before. The results are presented as shown in Fig. 12. As can be seen, the effect of the slotted bridge has resulted in a dramatic increase in the suppression band of the filter, with almost 2 GHz band of signal rejection when compared with the filter without the slotted line (see Fig. 9). Furthermore, the effect of the host dielectric material is noted to further miniaturize the bandstop filter as can be seen from Fig. 12.

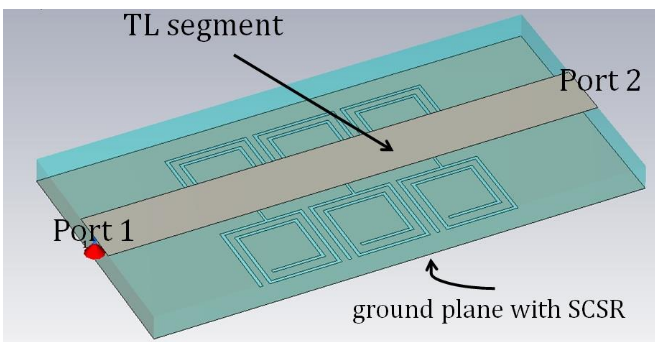


**Fig. 11** 3D view of the bandstop filter with slotted-complementary spiral resonators etched out from metallic ground plane. Note that TL segment is matched to 50Ω.

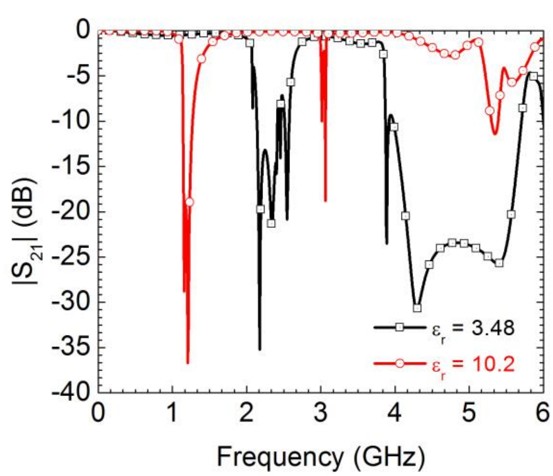


**Fig. 12** Simulated transmission coefficient, $S_{21}$, for the filter with slotted-CSRs (S-CSRs).

For this particular study, the effect of the dielectric material is considered with only two host media. Next, the current distribution for the filter with slotted-CSRs is shown in Fig. 13 at the SCSRs' resonant frequency of 2.1 GH, when dielectric medium ($\varepsilon_r$ = 3.48, tanδ = 0.002) is used.

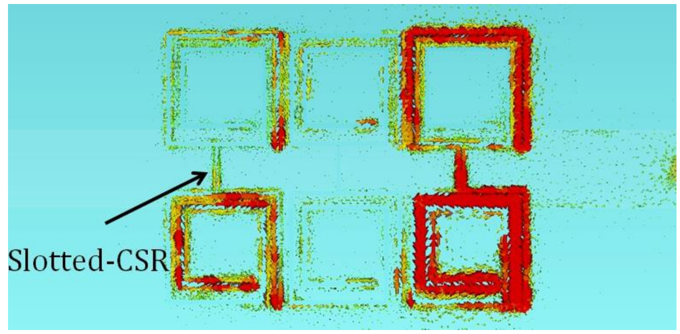


**Fig. 13** Snapshot for simulated surface current distribution along the vicinity of the metallic ground plane of the bandstop filter with Slotted-CSRs at resonant frequency of 2.1 GHz.

## 3 CONCLUSIONS

In this paper, bandstop filters based on developed slotted complementary split ring resonators and slotted complementary spiral resonators were proposed and investigated. The filters were numerically studied using full-wave time-domain simulator of CST Microwave Studio. Parametric studies based on varying the filter's geometrical parameters as well as the host dielectric medium were thoroughly conducted and several remarks based on the suppression band of the proposed filter were highlighted in the context of the discussed results.

## 4 ACKNOWLEDGMENT

The author would like to thank Sultan Qaboos University for providing the resources to accomplish this research work. The author also acknowledges the support from CST Microwave Studio for providing trials to do the full-wave modeling of the filters.

## 5 REFERENCES

[1] M. Mandal and P. Mondal, "Design of sharp-rejection, compact, wideband bandstop filters," *IET Microw. Antennas Propag.*, Vol. 2, No. 4, pp. 389-393, 2008.

[2] F. Yang, K. Ma, Y. Qian, and T. Itoh, "A uniplanar compact photonic-bandgap (UC-PBG) structure and its applications for microwave circuit," *IEEE Trans. Micro. Theory Tech.*, Vol. 47, No. 8, pp. 1509-1514, 1999.

[3] C. Hang, W. Deal, T. Qian, and T. Itoh, "High efficiency transmitter front-ends integrated with planar an PBG," *Asia-Pacific Microwave Conf. Dig.*, pp. 888-894, Dec. 2000.

[4] A. Safwat, F. Podevin, P. Ferrari, and A. Vilcot, "Tunable band-strop defected ground structure resonator using reconfigurable dumbbell-shaped coplanar waveguide," *IEEE Trans. Microw. Theory Tech.*, Vol. 54, No. 9, pp. 3559-3564, Sep. 2006.

[5] X. Chen, X. Shi, Y. Guo, and M. Xiao, "A novel dual band transmitter using microstrip defected ground structure," *Progress In Electromagnetics Research*, Vol. 83, pp. 1-11, 2008.

[6] R. Marques, F. Martin, and Sorolla, M., Metamaterials with negative parameters: theory, design and microwave applications, *John Wiley and Sons Inc.*, 2008.

[7] R. Marques, F. Mesa, J. Martel, and F. Medina, "Comparative analysis of edge- and broadside- coupled split ring resonators for metamaterial design - theory and experiments," *IEEE Transactions on Antennas Propagation*, Vol. 51, Issue 10, pp. 2572-2581, Oct. 2003.

[8] J. Bonache, M. Gil, I. Gil, J. Garcia-Garcia, and F. Martin, "On the electrical characteristics of complementary metamaterial resonators," *IEEE Microwave Wireless Components Letters*, Vol. 16, Issue 10, pp. 543-545, Oct. 2006.

[9] J.B. Pendry, A.J. Holden, D.J. Robbins, and W.J. Stewart, "Magnetism from conductors and enhanced nonlinear phenomena," *IEEE Transactions on Microwave Theory Techniques*, Vol. 47, Issue 11, pp. 2075–2084, Nov 1999.

[10] D. R. Smith, W. Padilla D. Vier, S. Nemat-Nasser, S. Schultz, "Composite medium with simultaneously negative permeability and permittivity," *Phys. Rev. Lett.*, 84, No. 18, pp. 4184, May 2000.

[11] V. Veselago, "The electrodynamics of materials with negative permittivity and negative permeability," *Soviet Physics USPEKI*, 10, 509, 1968.

[12] F. Falcone, T. Lopetegi, J.D. Baena, R. Marques, F. Martin, and M. Sorolla, "Effective negative-ε stopband microstrip lines based on complementary split ring resonators," *IEEE Microwave Wireless Components Letters*, Vol. 14, Issue 6, pp. 280-282, 2004.

[13] F. Falcone, T. Lopetegi, M. A. G. Laso, J. D. Baena, J. Bonache, M. Beruete, R. Marqu´es, F. Martın, and M. Sorolla, "Babinet principle applied to the design of metasurfaces and metamaterials," *Phys. Rev. Lett.*, Vol. 93, No. 19, pp. 197401-197404, Nov 2004.

[14] M.M. Bait-Suwailam, O.F. Siddiqui, and O.M. Ramahi, "Mutual coupling reduction between microstrip patch antennas using slotted-complementary split-ring resonators," *IEEE Antenna Wireless Propagation Letters*, Vol. 9, pp. 876-878, 2010.

[15] M. M. Bait-Suwailam, "Numerical study of bandstop filters based on slotted-complementary split-ring resonators (SCSRRs)," *in the second international conference of technological advances in electrical, electronics and computer engineering*, pp. 34 – 37, Kuala Lumpur, Malaysia, March 18-20.

[16] J. Garcia-Garcia, F. Martin, F. Falcone, J. Bonache, J.D. Baena, I. Gil, E. Amat, T. Lopetegi, M.A.G. Laso, J.A.M. Iturmendi, M. Sorolla, and R. Marques, "Microwave filters with improved stopband based on sub-wavelength resonators," *IEEE Trans. Microw. Theory Tech.*, Vol. 53, No. 6, pp. 1997-2006, June 2005.